

Hydration Structure of SCN^- in Concentrated Aqueous Sodium Thiocyanate Solutions

Yasuo KAMEDA,* Ryuji TAKAHASHI, Takeshi USUKI, and Osamu UEMURA

Department of Chemistry, Faculty of Science, Yamagata University, Kojirakawa-machi 1-4-12, Yamagata 990

(Received October 15, 1993)

Time-of-flight (TOF) neutron-diffraction measurements for 10 mol% NaSC^{14}N and NaSC^{15}N solutions in D_2O were carried out in order to investigate the hydration structure around the thiocyanate ion, SCN^- . There are 1.8 ± 0.2 water molecules coordinated to SCN^- with an intermolecular distance of $r(\text{N} \cdots \text{D}) = 2.16 \pm 0.02$ Å, suggesting that the hydrogen bond is formed between SCN^- and the nearest-neighbor water molecules. It has also been indicated by pairing the neutron-diffraction and X-ray diffraction results that the angle between the molecular axis of SCN^- and the hydrogen bond, $\angle \text{C-N} \cdots \text{H}_2\text{O}$, is ca. 120° in 10 and 20 mol% NaSCN aqueous solutions. Furthermore, details concerning the local structure around Na^+ in these concentrated solutions have been proposed based on the results of a least-squares fitting between the observed and structural model functions.

Considerable efforts have hitherto been made to elucidate the structural geometry concerning the complex formation of the thiocyanate ion (SCN^-) with various metal ions. Structural studies of these metal complexes have focused on the ambidentate nature of SCN^- .¹⁾ For example, according to recent X-ray diffraction and Raman spectroscopic studies for both aqueous²⁾ and dimethyl-sulfoxide³⁾ solutions, SCN^- coordinates tetrahedrally with Zn^{2+} through the nitrogen atom, and, on the other hand, Hg^{2+} is attached to four sulfur atoms in the first coordination sphere. However, despite the many structural studies for solutions containing SCN^- , very little information concerning the hydration structure of SCN^- itself, is known, due to the following reasons. One is that since the total structure factor of aqueous solutions obtained by the conventional type X-ray diffraction experiment is mainly dominated by water–water correlations, due to the overwhelming number of water molecules, it is difficult to pick up exact correlations between SCN^- and water molecules. Secondly, it is more difficult to determine the orientational configuration between an ion and its surrounding water molecules by X-ray diffraction alone, because of the extremely weak scattering factor of the hydrogen atom. In this respect, neutron diffraction is one of the most powerful experimental techniques. Particularly, neutron diffraction with isotopic substitution can supply quantitative information concerning the local structure around the isotopically substituted atom.

In the present paper we describe the results of TOF neutron diffraction and X-ray diffraction experiments for concentrated aqueous NaSCN solutions. The isotopic difference function from the neutron diffraction ($\Delta_N(Q)$) between two solutions, $(\text{NaSC}^{14}\text{N})_{0.1}(\text{D}_2\text{O})_{0.9}$ and $(\text{NaSC}^{15}\text{N})_{0.1}(\text{D}_2\text{O})_{0.9}$, provides direct information regarding SCN^- hydration. Further, the structural parameters for Na^+ hydration can be deduced in combination with the interference function from the X-ray diffraction, together with the network feature between hydrogen-bonded solvent molecules in this solution.

Experimental

Neutron Diffraction Measurement. Isotopically enriched NaSC^{15}N (99.0% ^{15}N) obtained from CIL Inc. and natural NaSCN (99.6% ^{14}N) of guaranteed grade (Nacalai Tesque), which were both dried in vacuo, were dissolved into D_2O (99.8% D, Merck Inc.) to prepare two 10 mol% NaSCN aqueous solutions with different isotopic compositions of nitrogen atoms. Both solutions were selected in the neutron-diffraction measurement. The TOF neutron-diffraction measurement for a sample solution sealed in a cylindrical quartz cell (8 mm in inner diameter and 0.4 mm in thickness) was carried out at 25°C using the HIT spectrometer⁴⁾ installed at the pulsed spallation neutron source (KENS) at the National Laboratory for High Energy Physics, Tsukuba, Japan. Scattered neutrons were detected by ^3He counters located at respective scattering angles of $2\theta = 8, 14, 25, 32, 44, 91$ and 150° . The time of data accumulation in the measurement was ca. 8 h for both solutions. The scattering intensities were measured in advance for an empty cell, background and a vanadium rod having the same dimensions as those of the sample.

X-Ray Diffraction Measurement. X-Ray diffraction measurements for 10 and 20 mol% NaSCN aqueous solutions were made at 25°C in the reflection geometry using a θ – θ X-ray diffractometer, manufactured by Rigaku Co. The isotopic compositions of the constituent atoms in the sample are all the natural abundance. The sample was put in a flat tray of poly(vinyl chloride) with surface dimensions of 150×20 mm² and 20 mm deep. The tray was filled with the sample and covered semi-circularly with a thin polyethylene film in order to prevent the solution from evaporation. The $\text{Mo } K\alpha$ radiation ($\lambda = 0.7107$ Å) produced from a Rigaku A-41L-Mo tube (operated at 50 kV and 35 mA) was employed for the diffraction measurement. A focusing graphite monochromator was placed in the reflected beam in order to reduce the $K\beta$ radiation, Compton and background intensities. The vertical beam divergence was limited through 1° divergence slits. The scattered intensity was counted at an interval of 0.2° over the range of $3 \leq 2\theta \leq 150^\circ$, corresponding to the scattering vector range, $0.5 \leq Q \leq 17.1$ Å⁻¹ ($Q = 4\pi \sin \theta / \lambda$), with a fixed counting time of 40 s. The whole angular range was scanned four times in order to minimize any long-term instrumental drift. The total number

Table 1. Isotopic Compositions and Mean Scattering Lengths b_N of Nitrogen Atoms, Mean Scattering and Absorption Cross Sections and the Number Densities Scaled in the Stoichiometric Unit $(\text{NaSCN})_{0.1}(\text{D}_2\text{O})_{0.9}$, σ_s , σ_a , and ρ , Respectively, for the Sample Used in the Neutron Diffraction Measurement

Samples	$^{14}\text{N}/\%$	$^{15}\text{N}/\%$	$b_N/10^{-12}$ cm	σ_s/barns	$\sigma_a/\text{barns}^a)$	$\rho/\text{\AA}^{-3}$
NaSC^{14}N	99.6	0.4	0.936	19.701	0.297	0.0294
NaSC^{15}N	1.0	99.0	0.649	19.080	0.109	

a) For the incident wavelength of 1.8 Å.

of counts was at least 80000 counts, and ranged over as high as 1500000 counts.

Data Reduction

Neutron Diffraction Data. The measured scattering intensities for 10 mol% NaSC^{14}N and NaSC^{15}N solutions were corrected for the background intensity, absorption of both the sample and cell,⁵⁾ as well as multiple⁶⁾ and incoherent scatterings. The sample parameters used are listed in Table 1. The coherent scattering length as well as the scattering and absorption cross sections for the constituent nuclei were, respectively, taken from those tabulated by Sears.⁷⁾ The observed count rate of the sample was converted to the absolute scale by using the scattering intensities from a vanadium rod. The first-order difference function⁸⁾ ($\Delta_N(Q)$) was determined based on the numerical difference in the normalized scattering cross section between both solutions. The inelasticity effect, mainly arising from a self-scattering contribution of deuterium atoms, is expected to sufficiently disappear in the term of $\Delta_N(Q)$, even at a large scattering angle, such as $2\theta = 91^\circ$,^{8,9)} through the subtracting process of two scattering data sets in which the inelasticity distortion is identically included. $\Delta_N(Q)$ s obtained experimentally at scattering angles of 14, 25, 41, and 91° , which agree well each other, were combined for the subsequent data analyses. The whole functional form of $\Delta_N(Q)$ for the 10 mol% NaSCN aqueous solution was thus determined, which is given in Fig. 1a.

$\Delta_N(Q)$ for the NaSCN aqueous solution can be represented by a linear combination of the following six partial structure factors concerning the nitrogen atom, i.e.:

$$\Delta_N(Q) = A[a_{\text{NO}}(Q) - 1] + B[a_{\text{ND}}(Q) - 1] + C[a_{\text{NC}}(Q) - 1] + D[a_{\text{NS}}(Q) - 1] + E[a_{\text{NNa}}(Q) - 1] + F[a_{\text{NN}}(Q) - 1],$$

where

$$\begin{aligned} A &= 2c_{\text{NCO}}b_{\text{O}}(b_{14\text{N}} - b_{15\text{N}}), B = 2c_{\text{NCD}}b_{\text{D}}(b_{14\text{N}} - b_{15\text{N}}), \\ C &= 2c_{\text{NCC}}b_{\text{C}}(b_{14\text{N}} - b_{15\text{N}}), D = 2c_{\text{NCS}}b_{\text{S}}(b_{14\text{N}} - b_{15\text{N}}), \\ E &= 2c_{\text{NcNa}}b_{\text{Na}}(b_{14\text{N}} - b_{15\text{N}}), F = c_{\text{N}}^2(b_{14\text{N}}^2 - b_{15\text{N}}^2), \end{aligned} \quad (1)$$

and c_i is the number of atom i in the stoichiometric unit $(\text{NaSCN})_{0.1}(\text{D}_2\text{O})_{0.9}$. The value of weighting factors (A, B, C, D, E , and F) is numerically summarized in

Table 2. Values of the Coefficients of $a_{ij}(Q)$ in Eq. 1

A/barns	B/barns	C/barns	D/barns	E/barns	F/barns
0.0302	0.0694	0.0038	0.0016	0.0021	0.0046

Table 2.

The Fourier transform of $\Delta_N(Q)$ corresponds to the distribution function around the nitrogen atom ($\bar{G}_N(r)$), the result of which is shown in Fig. 2a. Here,

$$\begin{aligned} \bar{G}_N(r) &= 1 + (A + B + C + D + E + F)^{-1} \\ &\quad \times (2\pi^2 \rho r)^{-1} \int_0^{Q_{\text{max}}} Q \Delta_N(Q) \sin(Qr) dQ \\ &= [Ag_{\text{NO}}(r) + Bg_{\text{ND}}(r) + Cg_{\text{NC}}(r) + Dg_{\text{NS}}(r) \\ &\quad + Eg_{\text{NNa}}(r) + Fg_{\text{NN}}(r)] \\ &\quad \times (A + B + C + D + E + F)^{-1}, \end{aligned} \quad (2)$$

where ρ is the number density of the sample. Since terms A and B of Eq. 2 are much larger than C, D, E , and F , $\bar{G}_N(r)$ is almost dominated by the nitrogen-water correlations. The coordination number of atom α around atom N($n_{\text{N}\alpha}$) in the range between r_1 and r_2 is given by

$$n_{\text{N}\alpha} = 4\pi c_{\alpha} \rho \int_{r_1}^{r_2} r^2 \bar{G}_N(r) dr \cdot \frac{A + B + C + D + E + F}{A_{\alpha}}, \quad (3)$$

where A_{α} denotes the weighting factor of the N- α pair.

X-Ray Diffraction Data. The observed scattering intensities of the X-ray diffraction were corrected for the background, polarization,¹⁰⁾ absorption,¹¹⁾ and double scattering,¹²⁾ respectively. Analytical expressions of the coherent scattering factors and incoherent intensities for the Na, S, C, N, and O atoms and for H_2O molecule were referred from a paper of Hajdu,¹³⁾ and the coherent scattering factor for H atom was taken from a paper of Stewart et al.¹⁴⁾ The values of the anomalous dispersion coefficients for all related atoms were adopted from a table of Cromer and Liberman.¹⁵⁾ The absolute scale for the scattering intensities was established using a method described by Habenschuss and Spedding.¹⁶⁾ The observed total interference term ($i^{\text{obs}}(Q)$) is given below:¹⁷⁻¹⁹⁾

$$i^{\text{obs}}(Q) = (I_{\text{eu}}(Q) - \langle f^2 \rangle) / \langle f \rangle^2$$

where

$$\langle f^2 \rangle = \sum c_i [(f_i(Q) + f'_i)^2 + f''_i^2]$$

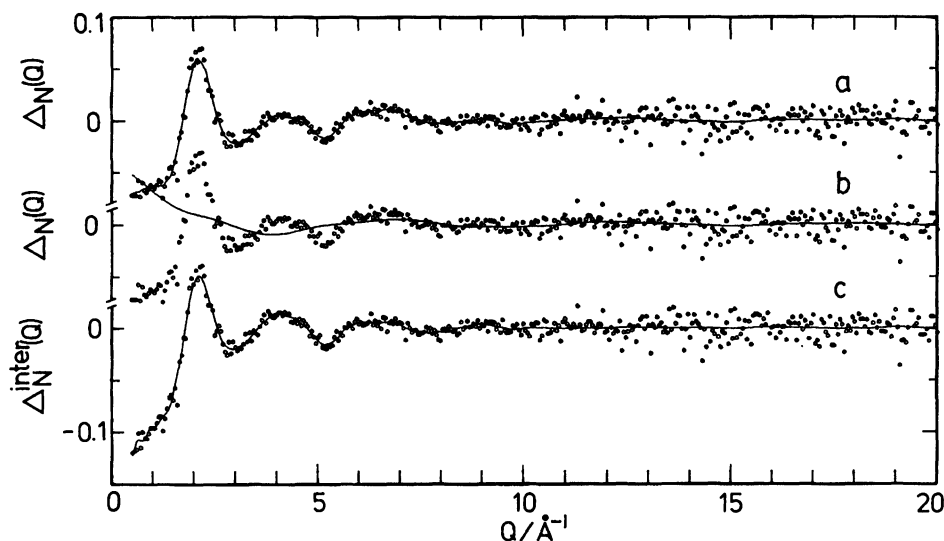


Fig. 1. a) Circles: The observed difference function, $\Delta_N(Q)$, for the 10 mol% NaSCN solution in D_2O . Solid line: Smoothed $\Delta_N(Q)$ used for the Fourier transform (Fig. 2a). b) Circles: The observed $\Delta_N(Q)$. Solid line: $I^{\text{intra}}(Q)$ based on intramolecular N-C and N...S contributions. c) Circles: The intermolecular contribution, $\Delta_N^{\text{inter}}(Q)$. Solid line: The back transform of $\bar{G}_N^{\text{inter}}(r)$ shown in Fig. 2b.

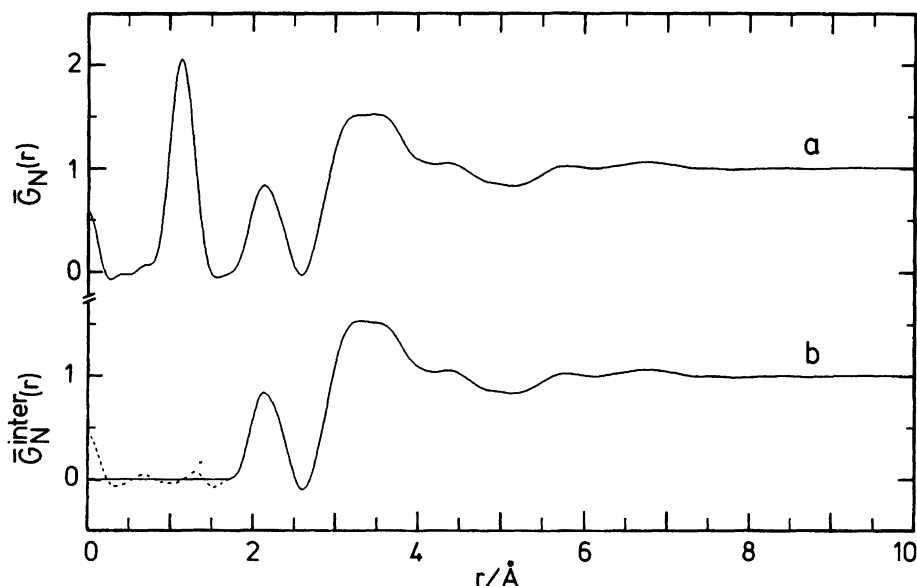


Fig. 2. a) The total and b) intermolecular distribution functions around the nitrogen atom, $\bar{G}_N(r)$ and $\bar{G}_N^{\text{inter}}(r)$, truncated at $Q_{\text{max}} = 20.0 \text{ \AA}^{-1}$, for the 10 mol% NaSCN solution in D_2O .

and

$$\langle f \rangle^2 = [\sum c_i [(f_i(Q) + f'_i)]^2 + [\sum c_i f''_i]^2]. \quad (4)$$

Here, $I_{\text{eu}}(Q)$ expresses the normalized coherent scattering intensity in electron units and $f_i(Q)$ corresponds to the atomic scattering factor of atom i . The real and imaginary parts for the anomalous dispersion factor are denoted by f'_i and f''_i , respectively. The radial distribution function ($G(r)$) is evaluated by the Fourier transform of $i(Q)$ according to the following equation:

$$G(r) = 1 + \frac{1}{2\pi^2 \rho r} \int_0^{Q_{\text{max}}} Q i(Q) \sin(Qr) dQ. \quad (5)$$

The upper limit of the integral (Q_{max}) in the present measurement was set to be 17.1 \AA^{-1} . The theoretical interference function ($i^{\text{calc}}(Q)$) due to all possible atom pairs in the system is expressed as

$$i^{\text{calc}}(Q) = \sum i_{ij}(Q),$$

where

$$i_{ij}(Q) = 2c_i n_{ij} \{ (f_i(Q) + f'_i)(f_j(Q) + f'_j) + f''_i f''_j \}$$

$$\times \exp(-l_{ij}^2 Q^2/2) \frac{\sin Qr_{ij}}{Qr_{ij}} / < f >^2. \quad (6)$$

Here, n_{ij} , l_{ij} , and r_{ij} are the coordination number, root-mean-square displacement and interatomic distance of the i - j pair, respectively. The values are determined by a least-squares fit of Eq. 6 to $i^{\text{obs}}(Q)$ in the $6.0 \leq Q \leq 17.1 \text{ \AA}^{-1}$ range. The fitting was performed using the SALS program,²⁰⁾ assuming that any statistical errors distribute uniformly over the entire range of the Q covered.

Results and Discussion

The sharp first peak located at $r \approx 1.2 \text{ \AA}$ in $\overline{G}_N(r)$ (Fig. 2a) is assigned to the intramolecular N-C interaction within SCN^- . The peak position, $r_{\text{NC}} = 1.16 \pm 0.02 \text{ \AA}$, and the coordination number, $n_{\text{NC}} = 1.0 \pm 0.2$, were respectively determined from a Gaussian fit of the first peak in $r\overline{G}_N(r)$ curve in the range of $0.7 \leq r \leq 1.48 \text{ \AA}$. This intramolecular N-C distance is in good agreement with those reported for crystalline NaSCN ($1.17 \pm 0.02 \text{ \AA}$),²¹⁾ crystalline KSCN ($1.170 \pm 0.006 \text{ \AA}$)²²⁾ and molten KSCN (1.15 \AA).²³⁾ The closeness of the magnitude of n_{NC} to the expected value ($n_{\text{NC}} = 1$) evidences the reasonableness of the present correction and normalization procedures for the diffraction intensities. The second peak, located at $r \approx 2.2 \text{ \AA}$, may possibly be ascribed to an intermolecular N...D interaction between SCN^- and the surrounding water molecules in the first hydration shell of the anion, since the intramolecular N...S peak should appear at a longer distance, $r = 2.8 \text{ \AA}$,²¹⁻²³⁾ and, in addition, its peak area of $n_{\text{NS}} = 1$ may be expected to be much smaller due to the relatively small scattering length of the S atom.

The intramolecular contribution for N-C and N...S pairs in Q -space ($I^{\text{intra}}(Q)$) is theoretically defined as

$$I^{\text{intra}}(Q) = 2c_N b_C (b_{14N} - b_{15N}) \exp(-l_{\text{NC}}^2 Q^2/2) \frac{\sin Qr_{\text{NC}}}{Qr_{\text{NC}}} + 2c_N b_S (b_{14N} - b_{15N}) \exp(-l_{\text{NS}}^2 Q^2/2) \frac{\sin Qr_{\text{NS}}}{Qr_{\text{NS}}}. \quad (7)$$

We then evaluated $I^{\text{intra}}(Q)$ employing the values $l_{\text{NC}} = 0.062 \text{ \AA}$, $l_{\text{NS}} = 0.065 \text{ \AA}$, and $r_{\text{NS}} = 2.80 \text{ \AA}$, obtained from TOF neutron data for molten KSCN by Ohno et al.,²³⁾ and $r_{\text{NC}} = 1.16 \text{ \AA}$ taken from the first peak of the present $\overline{G}_N(r)$, the result of which is depicted by the solid line in Fig. 1b. Perhaps, these structural parameters can be determined from least-squares fits of Eq. 7 to the present $\Delta_N(Q)$ observed in the high- Q region.^{24,25)} However, it seems to be difficult to extract reliable values of these structural parameters by this method because of the limited statistical accuracy of the present data-points of $\Delta_N(Q)$ in the region $Q \geq 10 \text{ \AA}^{-1}$. The Fourier transform of the difference function in Q -space, $\Delta_N^{\text{inter}}(Q)$ (Fig. 1c), obtained by subtracting the theoretical $I^{\text{intra}}(Q)$ from the observed $\Delta_N(Q)$, gives the intermolecular distribution function, $\overline{G}_N^{\text{inter}}(r)$ (Fig. 2b), which reflects the distribution of water molecules around the nitrogen atom of SCN^- . The structural parameters for the nearest-

neighbor N...D interaction, $r_{\text{N...D}} = 2.16 \pm 0.02 \text{ \AA}$ and $n_{\text{N...D}} = 1.8 \pm 0.2$, are deduced from a Gaussian fit of the $r\overline{G}_N^{\text{inter}}(r)$ curve in the range of $1.73 \leq r \leq 2.50 \text{ \AA}$. The value of $r_{\text{N...D}}$ is much smaller than the sum of the van der Waals radii of nitrogen and hydrogen atoms (2.8 \AA), implying the formation of a hydrogen bond between SCN^- and the nearest-neighbor water molecules. Assuming a liner configuration of the hydrogen-bonded, N...D-O_w, intermolecular distances between the nitrogen atom and the oxygen atom in the neighboring water molecule, $r_{\text{N...O}_w}$, and between the nitrogen atom and another deuteron atom belonging to the same water molecule, $r_{\text{N...D}'}$, are respectively calculated to be 3.14 and 3.50 \AA , with the aid of the molecular geometry well-known for D_2O molecules in the liquid state.^{26,27)} These contributions seem to be included in the broad peak centered at $r \approx 3.5 \text{ \AA}$ in $\overline{G}_N^{\text{inter}}(r)$. The integration from $r = 1.73$ to 4.20 \AA indicates that there exist 8.8 water molecules in this region, suggesting that about 7 water molecules lie in the broadened coordination region centered at $r \approx 3.5 \text{ \AA}$.

Figures 3 and 4 exhibit the total interference term ($i(Q)$) and the corresponding distribution function ($G(r)$) for the 10 mol% NaSCN solution from X-ray diffraction data, respectively. Four main peaks in the experimental $G(r)$ can be observed at about 0.8–1.2, 1.7, 2.4, and 2.8 \AA with a small hump at 3.2 \AA . A broadened feature also appears around 7 \AA . The peak at 0.8–1.2 \AA can be reasonably ascribed to the intramolecular O-H interaction within the H_2O molecule and the intramolecular N-C one within SCN^- , respectively. The peak at 1.7 \AA corresponds to the intramolecular C-S interaction within SCN^- . The peak at 2.4 \AA may be

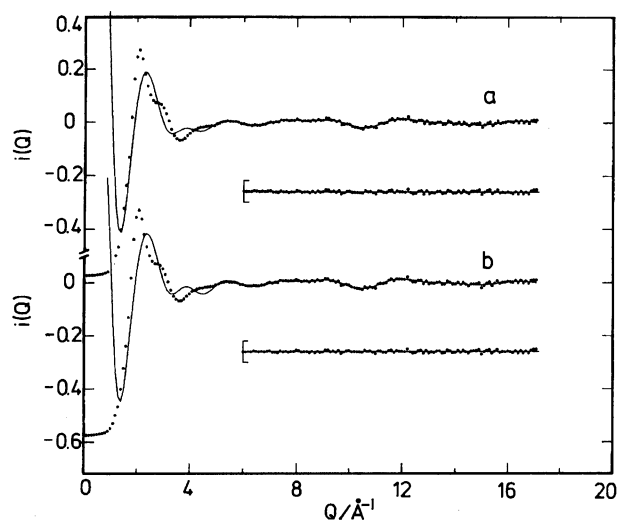


Fig. 3. Circles: The observed X-ray total interference term, $i^{\text{obs}}(Q)$, for the 10 mol% NaSCN solution in H_2O (a and b). Solid line: the calculated interference terms, $i^{\text{calc}}(Q)$, with (a) $n_{\text{Na...H}_2\text{O}} = 4$ and (b) $n_{\text{Na...H}_2\text{O}} = 6$, respectively. The differences between $i^{\text{obs}}(Q)$ and $i^{\text{calc}}(Q)$ at $Q > 6 \text{ \AA}^{-1}$ are shown below.

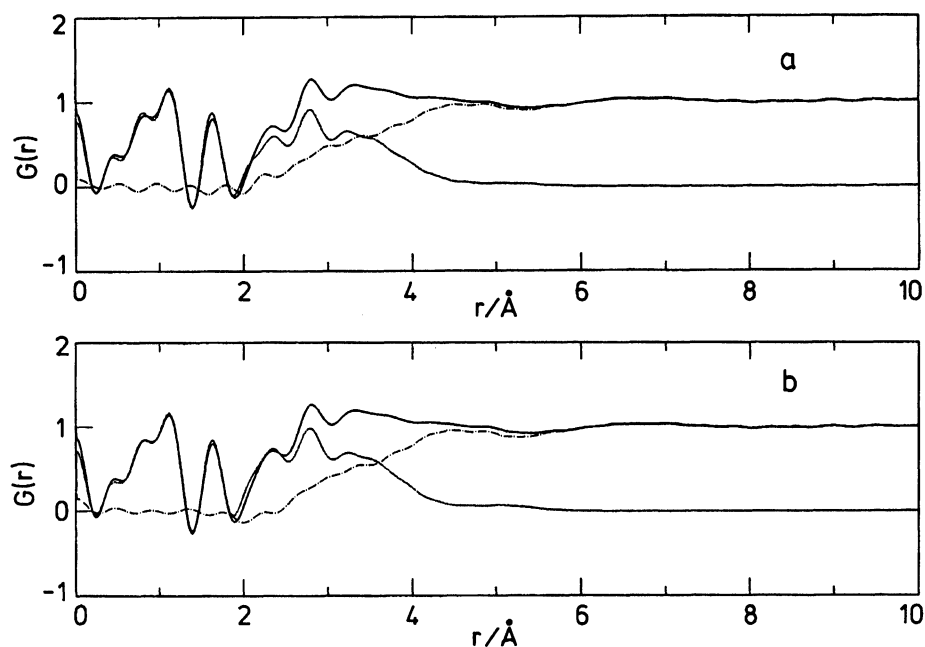


Fig. 4. The solid line: The observed X-ray total distribution function, $G(r)$, for the 10 mol% NaSCN solution in H_2O (a and b). Dotted line: The calculated distribution function, $G^{\text{calc}}(r)$, with (a) $n_{\text{Na}\cdots\text{H}_2\text{O}}=4$ and (b) $n_{\text{Na}\cdots\text{H}_2\text{O}}=6$, respectively. Dashed-dot line: The Fourier transform of the difference, $i^{\text{obs}}(Q)-i^{\text{calc}}(Q)$, for (a) $n_{\text{Na}\cdots\text{H}_2\text{O}}=4$ and (b) $n_{\text{Na}\cdots\text{H}_2\text{O}}=6$, respectively.

attributed to the nearest-neighbor $\text{Na}^+\cdots\text{H}_2\text{O}$ interaction for the following reasons: (1) This peak position is almost identical to the sum of the ionic radius of Na^+ and the effective radius of a water molecule in aqueous solutions.²⁷⁾ (2) The nearest-neighbor intermolecular distance for the $\text{H}_2\text{O}\cdots\text{H}_2\text{O}$ interaction, 2.8–2.9 Å,^{16–18)} reported for various aqueous solutions, is sufficiently far from this position. (3) The nearest-neighbor distance for the $\text{SCN}^-\cdots\text{H}_2\text{O}$ interaction, $r_{\text{N}\cdots\text{O}_w}$, is suggested to be 3.14 Å based on an analysis of the present neutron data. The 2.8 Å peak in $G(r)$ is considered to include the hydrogen-bonded $\text{H}_2\text{O}\cdots\text{H}_2\text{O}$ interaction, and possibly the intramolecular S \cdots N interaction within SCN^- . The small hump in $G(r)$ at 3.2 Å may be connected with the nearest-neighbor nitrogen atom \cdots water molecule correlation in solution.

We next carried out a least-squares fit for $i(Q)$ on the basis of information obtained from the experimental $G(r)$ and determine the structural parameters of the nearest-neighbor intermolecular correlations r_{ij} , l_{ij} , and n_{ij} , in both 10 and 20 mol% NaSCN aqueous solutions. We made the following assumptions when calculating the theoretical interference function, $i^{\text{calc}}(Q)$: (a) The intramolecular O–H and H–H distances, r_{OH} and r_{HH} , and their root mean square displacements, l_{OH} and l_{HH} , within the H_2O molecule are fixed at values reported previously for liquid D_2O .^{28,29)} (b) The intramolecular parameters for SCN^- , such as r_{NC} , r_{SC} , r_{NS} , l_{NC} , l_{SC} , and l_{NS} , are refined as an independent parameter. (c) The correlation between the Na^+ and H_2O molecules in the first hydration shell is introduced as below. The

intermolecular distance, $r_{\text{Na}\cdots\text{H}_2\text{O}}$, and its root-mean-square displacement, $l_{\text{Na}\cdots\text{H}_2\text{O}}$, are refined as an independent parameter. The fixed value of either 4 or 6 is assumed to be the coordination number, $n_{\text{Na}\cdots\text{H}_2\text{O}}$, in accordance with either the tetrahedral or octahedral hydration geometry of Na^+ , in order to determine the $\text{H}_2\text{O}\cdots\text{H}_2\text{O}$ distance of the coordination polyhedron surrounding the ion. (d) The structural parameters of the hydrogen-bonded interaction between the H_2O molecules, $r_{\text{H}_2\text{O}\cdots\text{H}_2\text{O}}$, $l_{\text{H}_2\text{O}\cdots\text{H}_2\text{O}}$, and $n_{\text{H}_2\text{O}\cdots\text{H}_2\text{O}}$, are also refined independently. (e) The nearest-neighbor $\text{SCN}^-\cdots\text{H}_2\text{O}$ interaction is taken into account as follows. The values of $r_{\text{N}\cdots\text{H}_2\text{O}}$, $l_{\text{N}\cdots\text{H}_2\text{O}}$, and the angle $\angle\text{C–N}\cdots\text{H}_2\text{O}$, ϕ are allowed to vary independently. The coordination number, $n_{\text{N}\cdots\text{H}_2\text{O}}$, is fixed at 1.8, which has already been given in the present neutron information. The second nearest-neighbor $\text{SCN}^-\cdots\text{H}_2\text{O}$ interaction, appearing around $r=3.5$ Å in $\overline{G}_{\text{N}}^{\text{inter}}(r)$, is also involved, considering the broad distribution of the H_2O molecules. In this result, the final values of all independent parameters can be summarized as in Table 3.

Figures 3 and 4 give $i^{\text{calc}}(Q)$ and its Fourier transform, $G^{\text{calc}}(r)$, in the 10 mol% NaSCN aqueous solution, calculated using the structural parameters given in Table 3, together with the corresponding experimental ones, $i^{\text{obs}}(Q)$ and $G^{\text{obs}}(r)$. A good agreement is obtained between the experimental and calculated curves from both structural models of tetrahedral and octahedral hydration models around Na^+ ; in other words, it seems impossible to determine a reliable value of $n_{\text{Na}\cdots\text{H}_2\text{O}}$ (4 or 6), based on the present analysis of

Table 3. Results of the Least-Squares Refinements for Both 10 and 20 mol% NaSCN Solutions^{a)}

Sample	Interaction	$r_{ij}/\text{\AA}$	$l_{ij}/\text{\AA}$	n_{ij}	$\phi/^\circ$ ^{b)}
10 mol% NaSCN $n_{\text{Na}+\dots\text{H}_2\text{O}}=4$	S-C	1.64(1)	0.06(2)	1 ^{c)}	122(15)
	N-C	1.16(2)	0.05(3)	1 ^{c)}	
	N \cdots S	2.79(3)	0.05(3)	1 ^{c)}	
	$\text{Na}^+\cdots\text{H}_2\text{O}$	2.38(4)	0.24(3)	4 ^{c)}	
	N $\cdots\text{H}_2\text{O}$	3.16(9)	0.24(3)	1.8 ^{c)}	
	$\text{SCN}^-\cdots\text{H}_2\text{O}$	3.2(2)	0.40(4)	5(3)	
	$\text{H}_2\text{O}\cdots\text{H}_2\text{O}$	2.86(5)	0.25(3)	1.1(3)	
10 mol% NaSCN $n_{\text{Na}+\dots\text{H}_2\text{O}}=6$	S-C	1.64(1)	0.06(2)	1 ^{c)}	122(15)
	N-C	1.15(2)	0.06(2)	1 ^{c)}	
	N \cdots S	2.78(3)	0.06(2)	1 ^{c)}	
	$\text{Na}^+\cdots\text{H}_2\text{O}$	2.38(3)	0.25(1)	6 ^{c)}	
	N $\cdots\text{H}_2\text{O}$	3.13(8)	0.20(3)	1.8 ^{c)}	
	$\text{SCN}^-\cdots\text{H}_2\text{O}$	3.5(4)	0.4(9)	4(5)	
	$\text{H}_2\text{O}\cdots\text{H}_2\text{O}$	2.87(5)	0.17(5)	1.0(4)	
20 mol% NaSCN $n_{\text{Na}+\dots\text{H}_2\text{O}}=4$	S-C	1.655(7)	0.080(8)	1 ^{c)}	117(13)
	N-C	1.15(1)	0.05(2)	1 ^{c)}	
	N \cdots S	2.79(2)	0.06(2)	1 ^{c)}	
	$\text{Na}^+\cdots\text{H}_2\text{O}$	2.41(2)	0.19(1)	4 ^{c)}	
	N $\cdots\text{H}_2\text{O}$	3.2(2)	0.2(1)	1.0(6)	
	$\text{SCN}^-\cdots\text{H}_2\text{O}$	3.49(9)	0.33(4)	3.9(8)	
	$\text{H}_2\text{O}\cdots\text{H}_2\text{O}$	2.94(8)	0.22(4)	1.7(4)	
20 mol% NaSCN $n_{\text{Na}+\dots\text{H}_2\text{O}}=6$	S-C	1.660(7)	0.080(8)	1 ^{c)}	117(8)
	N-C	1.15(1)	0.05(2)	1 ^{c)}	
	N \cdots S	2.81(2)	0.06(2)	1 ^{c)}	
	$\text{Na}^+\cdots\text{H}_2\text{O}$	2.40(1)	0.229(8)	6 ^{c)}	
	N $\cdots\text{H}_2\text{O}$	3.1(1)	0.21(5)	1.8(7)	
	$\text{SCN}^-\cdots\text{H}_2\text{O}$	3.8(3)	0.43(4)	7(3)	
	$\text{H}_2\text{O}\cdots\text{H}_2\text{O}$	2.81(6)	0.23(8)	1.9(4)	

a) Estimated standard deviations are given in the parentheses. b) The bond angle, $\angle\text{C-N}\cdots\text{H}_2\text{O}$. c) Fixed.

X-ray data in the 10 mol% NaSCN solution. It appears in Fig. 4 that the distribution feature in the range with $r < 4 \text{ \AA}$ in $G^{\text{obs}}(r)$ is satisfactorily reproduced using short-range interaction parameters in the structure model described above. This is also supported by the fact that the Fourier transform of the residual function, $i^{\text{obs}}(Q) - i^{\text{calc}}(Q)$, (dashed-dot lines in Figs. 4a and 4b) varies smoothly against r at $r < 4 \text{ \AA}$.

The intramolecular bond lengths and root-mean-square displacements within SCN^- obtained in the present analysis are identical to those found in the literature for some alkali thiocyanate in crystalline^{21,22)} and molten states²³⁾ within the experimental errors, which explains the linear molecular structure of SCN^- . Moreover, the value of r_{NC} is in good agreement with that from an analysis of $\overline{G}_{\text{N}}(r)$.

The $r_{\text{Na}\cdots\text{H}_2\text{O}} = 2.38 \text{ \AA}$ and $l_{\text{Na}\cdots\text{H}_2\text{O}} = 0.24\text{--}0.25 \text{ \AA}$ values for the hydration structure around Na^+ , which are in common given in the tetrahedral and octahedral geometries, agree well with previous X-ray diffraction results for aqueous solutions containing Na^+ .^{17,18,30-33)}

The intermolecular $\text{N}\cdots\text{H}_2\text{O}$ distance, $r_{\text{N}\cdots\text{H}_2\text{O}} = 3.13\text{--}3.16 \text{ \AA}$, within the hydrogen-bonded $\text{SCN}^-\cdots\text{H}_2\text{O}$

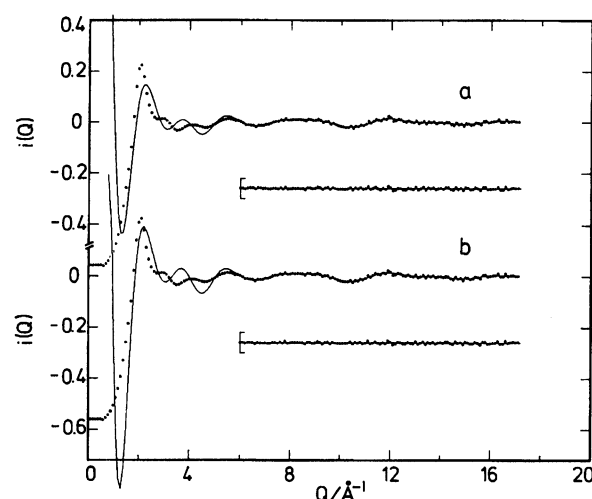


Fig. 5. Same notations as Fig. 3, except for the 20 mol% NaSCN solution.

interaction, corresponds well to the value, $r_{\text{N}\cdots\text{O}} = 3.14 \text{ \AA}$, obtained by the analysis for $\overline{G}_{\text{N}}^{\text{inter}}(r)$. The bond angle $\angle\text{C-N}\cdots\text{H}_2\text{O}$ can also be indicated to be $122 \pm 15^\circ$.

A least-squares fit for $i(Q)$ for the 20 mol% NaSCN so-

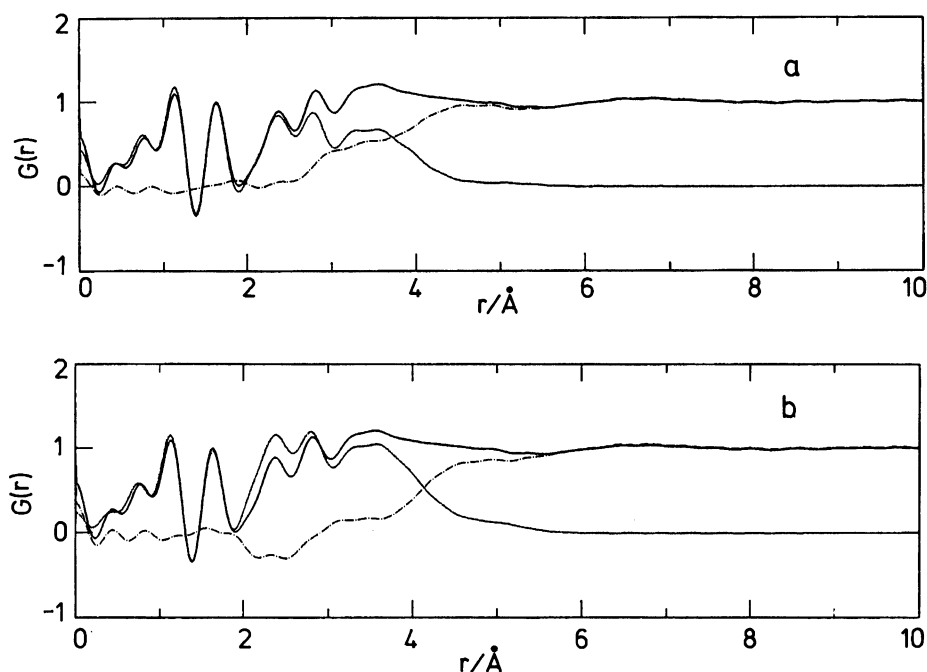


Fig. 6. Same notations as Fig. 4, except for the 20 mol% NaSCN solution.

lution was carried out using the same procedure as that applied for the 10 mol% NaSCN solution, except for the condition that the coordination number, $n_{\text{Na}\cdots\text{H}_2\text{O}}$, is allowed to vary as an independent parameter. The final results of the structural parameters for the 20 mol% NaSCN solution are given in Table 3. These parameters are very similar to the corresponding ones obtained for the 10 mol% NaSCN solution. Particularly, the agreement regarding the structural parameters of the $\text{SCN}^- \cdots \text{H}_2\text{O}$ correlations between 10 and 20 mol% NaSCN solutions suggests that a well-defined orientational correlation between SCN^- and the nearest-neighbor water molecules is established, even in such a concentrated aqueous solution (20 mol% NaSCN).

Analogously to the result for the 10 mol% NaSCN solution, it still remains regarding the 20 mol% NaSCN solution that the coordination number, $n_{\text{Na}\cdots\text{H}_2\text{O}}$, cannot be specified from a least-squares fit, because both parameters, $n_{\text{Na}\cdots\text{H}_2\text{O}}=4$ and 6, can give a similar good fit to $i^{\text{obs}}(Q)$ in Q -space at $6.0 \leq Q \leq 17.1 \text{ \AA}^{-1}$, as shown in Fig. 5. As mentioned above, the hydration number of Na^+ could not also be specified in terms of the Fourier transform of the residual function, $i^{\text{obs}}(Q) - i^{\text{calc}}(Q)$, in the 10 mol% NaSCN solution. In the case of the 20 mol% NaSCN solution, the tetrahedral model seems to be rather preferred, because the residual function of this model varies smoothly against r at $r < 4 \text{ \AA}$ and, particularly, does not contain any unphysical portion within this range (Fig. 6a). On the other hand, the octahedral model contains a marked negative area in the vicinity of $r \approx 2.5 \text{ \AA}$, in which the $\text{Na}^+ \cdots \text{H}_2\text{O}$ contribution is predominant (Fig. 6b). In any case, it may be concluded that it is a very difficult problem to decide the obvious

hydration number around Na^+ in the aqueous NaSCN solution.

The authors wish to thank Professors Masakatsu Misawa (Niigata University) and Toshiharu Fukunaga (Nagoya University) for their help during the course of neutron diffraction measurement. All of the calculations in the present work were performed using the ACOS S3600 computer at the Computing Center of Yamagata University.

References

- 1) K. Vrieze and G. van Koten, "Comprehensive Coordination Chemistry," ed by G. Wilkinson, Pergamon Press, New York (1987), Vol. 2, p. 225.
- 2) T. Yamaguchi, K. Yamamoto, and H. Ohtaki, *Bull. Chem. Soc. Jpn.*, **58**, 3235 (1985).
- 3) I. Persson, Å. Iverfeldt, and S. Åhrland, *Acta Chem. Scand., Ser. A*, **A35**, 295 (1981).
- 4) N. Watanabe, T. Fukunaga, T. Shinohe, K. Yamada, and T. Mizoguchi, "Proc. 4th International Collaboration on Advanced Neutron Sources (ICANS-IV) KEK, Tsukuba," ed by Y. Ishikawa et al., (1981), p. 539.
- 5) H. H. Paalman and C. J. Pings, *J. Appl. Phys.*, **33**, 2635 (1962).
- 6) I. A. Belch and B. L. Averbach, *Phys. Rev.*, **137**, A1113 (1965).
- 7) V. F. Sears, "Thermal-Neutron Scattering Length and Cross Sections for Condensed-Matter Research," Atomic Energy of Canada Ltd., AECL-8490, (1984).
- 8) A. K. Soper, G. W. Neilson, J. E. Enderby, and R. A. Howe, *J. Phys. C: Solid State Phys.*, **10**, 1793 (1977).
- 9) K. Ichikawa, Y. Kameda, T. Matsumoto, and M. Misawa, *J. Phys. C: Solid State Phys.*, **17**, L725 (1984).

- 10) Y. Waseda, "The Structure of Non-Crystalline Materials," MacGraw-Hill, New York (1980), p. 27.
 - 11) M. E. Milberg, *J. Appl. Phys.*, **29**, 64 (1958).
 - 12) B. E. Warren and R. L. Mozzi, *Acta Crystallogr.*, **21**, 459 (1966).
 - 13) F. Hajdu, *Acta Crystallogr., Sect. A*, **A28**, 250 (1972).
 - 14) R. F. Stewart, E. R. Davidson, and W. T. Simpson, *J. Chem. Phys.*, **42**, 3175 (1965).
 - 15) D. T. Cromer and D. Liberman, *J. Chem. Phys.*, **53**, 1891 (1970).
 - 16) A. Habenshuss and F. H. Spedding, *J. Chem. Phys.*, **70**, 2797 (1979).
 - 17) H. Ohtaki and N. Fukushima, *J. Solution Chem.*, **21**, 23 (1992).
 - 18) R. Caminiti, G. Licheri, G. Paschina, G. Piccaluga, and G. Pinna, *J. Chem. Phys.*, **72**, 4522 (1980).
 - 19) Y. Waseda, "Novel Application of Anomalous (Resonance) X-Ray Scattering for Structural Characterization of Disordered Materials," Springer-Verlag, New York (1984), p. 25.
 - 20) T. Nakagawa and Y. Oyanagi, "Recent Developments in Statistical Inference and Data Analysis," ed by K. Matushita, North-Holland (1980), p. 221.
 - 21) P. H. van Rooyen and J. C. A. Boeyens, *Acta Crystallogr., Sect. B*, **B31**, 2933 (1975).
 - 22) D. J. Cookson, M. M. Elecombe, and T. R. Finlayson, *J. Phys.: Condens. Matter*, **4**, 7851 (1992).
 - 23) H. Ohno, K. Igarashi, Y. Iwadate, M. Murofushi, J. Mochinaga, and K. Furukawa, *Proc. Electrochem. Soc.*, **86**, 296 (1986).
 - 24) Y. Kameda, H. Arakawa, K. Hangai, and O. Uemura, *Bull. Chem. Soc. Jpn.*, **65**, 2154 (1992).
 - 25) Y. Kameda, H. Saitoh, and O. Uemura, *Bull. Chem. Soc. Jpn.*, **66**, 1919 (1993).
 - 26) Y. Kameda and O. Uemura, *Bull. Chem. Soc. Jpn.*, **65**, 2021 (1992).
 - 27) Y. Marcus, *Chem. Rev.*, **88**, 1475 (1988).
 - 28) K. Ichikawa and Y. Kameda, *J. Phys.: Condens. Matter*, **1**, 257 (1989).
 - 29) K. Ichikawa, Y. Kameda, T. Yamaguchi, H. Wakita, and M. Misawa, *Mol. Phys.*, **73**, 79 (1991).
 - 30) M. Maeda and H. Ohtaki, *Bull. Chem. Soc. Jpn.*, **48**, 3755 (1975).
 - 31) G. Palinkas, W. O. Riede, and K. Heinzinger, *Z. Naturforsch., A*, **32a**, 1137 (1977).
 - 32) N. T. Skipper and G. W. Neilson, *J. Phys.: Condens. Matter*, **1**, 4141 (1989).
 - 33) R. Caminiti, F. Cilloco, and R. Felici, *Mol. Phys.*, **76**, 681 (1992).
-